APPLIED RESEARCH

Modeling Transient Cardiovascular Hemodynamics With Physiological Conscious Autoencoder

MEHMET ISCAN AND AYDIN YESILDIREK, (Member, IEEE)
Department of Mechatronics Engineering, Yıldız Technical University, 34349 Istanbul, Turkey

Corresponding author: Mehmet Iscan (miscan@yildiz.edu.tr)

ABSTRACT Current biomedical research relies primarily on in silico studies to model complex systems like cardiovascular hemodynamics. However, for comprehensive validation of mathematical models, real in vitro experiments are indispensable. This paper introduces a framework that bridges these approaches through the hybrid mock circulatory loop (hMCL), offering precise control, flexibility, and reproducibility. This innovation enables the investigation of cardiovascular disease mechanisms in a controlled setting, overcoming the limitations of live organism studies. The framework employs a modified autoencoder with a partially guided latent space, incorporating physiological insights into a deep neural network. It leverages time-delayed cardiovascular signals, including pressures, flow rates, and unmeasurable cardiovascular system (CVS) parameters, to estimate critical parameters like aortic and mitral resistance, systemic resistance, and left ventricle elastance. The autoencoder's loss function is tailored to predict these parameters, enhancing the understanding of cardiovascular dynamics. The study utilizes in silico data to train the model and validates it through in vitro tests using a hybrid mock loop device, yielding a remarkable accuracy of less than 5.7% error in replicating CVS signals. Furthermore, the framework demonstrates the adaptability of CVS variables to perturbations in closed-loop conditions and exhibits a diagnostic model with an impressive 98.55% F1 score for classifying cardiovascular disease severity. This research significantly advances the field by modifying the autoencoder to include physiological signals, introducing a novel loss function, developing a structured network, presenting a diagnostic model, and proposing an innovative approach for generating transient responses in cardiovascular hemodynamics, validated through in vitro and in silico experiments.

INDEX TERMS Aortic and mitral stenosis, cardiac contractility, CVS model parameter estimation, hMCL, physiological consciousness deep network, systemic resistance change.

I. INTRODUCTION

The cardiovascular system (CVS) plays a crucial role in the human body, and the prevalence of cardiovascular diseases (CVD) has increased due to lifestyle changes in the modern world. CVDs are responsible for approximately one-third of all deaths globally [1]. To address this issue, extensive research has been conducted to develop models for diagnosing, treating, and preventing cardiovascular

The associate editor coordinating the review of this manuscript and approving it for publication was Ganesh Naik.

abnormalities [2]. However, one of the challenges in analyzing, diagnosing, and treating CVD is the difficulty of non-invasively measuring cardiovascular signals from a live subject in real-time. The need to preserve the normal functioning of the cardiovascular system and comply with strict regulations imposed by authorities such as the FDA (Food and Drug Administration) and NCBI (National Center for Biotechnology Information) further complicates the process [3], [4]. Therefore, the development and utilization of effective CVS models are essential in addressing these challenges. These models can provide valuable insights into the

functioning of the cardiovascular system, help in early detection of abnormalities, guide treatment strategies, and aid in the development of preventive measures.

There are basically two common type of experiment to overcome these limitations: *in silico* and *in vitro* test. *In silico* refers to conducting experiments or simulations on a computer or through computational models, often used in fields like computer science and drug discovery, allowing researchers to analyze complex systems and predict outcomes [5]. On the other hand, *in vitro* involves conducting experiments in a controlled laboratory environment, typically using isolated biological components such as cells or tissues, or biomedical device that can be conditioned using software algorithm [14]. This method is crucial in biology and pharmacology to study biological processes and test the effects of various substances. While *in silico* is virtual and relies on data and algorithms, *in vitro* involves physical experiments with biological materials.

Model-based simulations and experiments are conducted to generate synthetic cardiovascular system (CVS) signals, which can be used for analyzing the CVS or emulating certain conditions for diagnostics and treatment of live subjects, such as aortic stenosis, heart failure, and more [5], [6], [7], [8]. Although, *in silico* tests offer complete knowledge of hemodynamic variables and parameters to interpret the nature of CVS, they are highly sensitive to assumptions made in mathematical modeling. That restricts model validity in a wide range of operation. To overcome such limitations of *in silico* test, the *in vitro* studies are conducted on physical analogous platforms for validation *in silico* models [9]. The mock loops (MCL) are an example of such devices filling the gap between clinical and engineering approaches. On the other hand, the hybrid mock loops (hMCL) enable us to access a richer set of CVS variables and parameters using either direct measurements or state estimation [9], [10]. This approach provides valuable insights into the behavior of the CVS and helps validate the assumptions made in mathematical models used for simulations. The combination of *in silico* and *in vitro* tests enhances our understanding of the cardiovascular system and aids in the development of more reliable diagnostic and treatment strategies.

The left ventricle (LV) pumping oxygenated blood to the body is a very critical section of CVS. Any deviation of its operation may have significant effects on the heart and other organs. Its characteristics are modeled by the pressure, the flow rate variables, and its elastance parameter. Together with resistances of aortic and mitral valves, they play a critical role in understanding the conditions of the CVS [11]. The modeling of the overall systemic cycle is completed with basic elements of fluid resistances, elastances and inertances in the closed-loop hemodynamic system. Although those signals coming from cyclic autonomous operation are periodic, they show dependency to a wide range of factors such as age, time, person to person, and other physiological conditions [12].

To accommodate such variations, different simplistic yet powerful models are suggested in various details, e.g., [5]. Experimental setups reproducing cardiac functions and *in vitro* data are essential for clinical studies. Such a system validating the dynamic behavior using in vivo data obtained from MRA is given in [13].

Data-driven models utilize machine learning and statistical techniques to learn patterns and relationships from cardiovascular data. These models can be trained on large datasets and used to make predictions, classify diseases, or estimate physiological parameters. They offer flexibility in capturing complex dynamics and individual variations in the cardiovascular system provided that a rich dataset is available. They have used data coming from both *in silico* and *in vitro* tests during the last couple of decades [14], [15], [16]. Such algorithms are utilized for the identification and prediction of the CVD and their treatment options to the experts [17].

In recent years, there have been many studies published related to estimation of CVS parameters especially for end-systolic left ventricular elastance (E_{LV}) and vascular resistance (R_{SYS}) which are the basic indicators watched for heart failure and systemic problems [18], [19]. Most of the studies focus on the estimation of the (E_{LV}) using the physiological data that can be measured invasively or noninvasively [20], [21], [22]. In general, the principal pressure and/or flow rate variables of CVS are considered in model development for heart failure or deprecated contractility, e.g. [23]. When a complete state-space is not measurable, extended Kalman filter methods are utilized for the measurement from real patients, some devices such as Left Ventricular Assisted Device (LVAD), or an artificial heart [22], [24], [25].

In this paper, the authors propose a novel framework based on a deep neural network (deepnet) for modeling, estimating key parameters of the cardiovascular system, and diagnosing certain cardiovascular diseases. The deepnet is constructed by a novel autoencoder called the physiologically conscious autoencoder (PCAE) is trained on a dataset generated by a five-state "principal" variable CVS model. The dataset used for training the deepnet is produced from different operations, including a healthy heart condition with varying left ventricular elastance values, aortic stenosis simulated by manipulating the aortic resistance, mitral stenosis mimicked by adjusting the mitral resistance, and varying systemic vascular resistances. By training the deepnet on this dataset, the authors aim to generalize the relationships between the CVS signals and these conditions. The autoencoder, which is a type of neural network architecture frequently used for dimensionality reduction and feature extraction, is modified to incorporate additional physiological signals into the latent space. These additional signals, referred to as "critical parameters," represent key CVS parameters. By including these critical parameters in the PCAE model, the authors not only create a model for the CVS but also estimate these important parameters. In addition to modeling and parameter estimation, the authors employ another deepnet model for

the classification of healthy hearts and different severities of CVDs, including aortic stenosis, mitral stenosis, and systemic vascular resistance. This classification model utilizes the learned features from the PCAE model to classify the different cardiovascular conditions. Furthermore, the authors demonstrate that perturbing a critical parameter in the PCAE model results in the corresponding adjustments in the CVS principal variables. This indicates that the PCAE model is able to reproduce the behavior of the CVS based on the variation of critical parameters. Finally, all signals from the proposed framework: the principal variables, the critical parameters, the diagnostics, have been compared *to in vitro* data obtained from the hMCL that authors developed [10].

The primary contributions of this study encompass several key aspects: 1) The modification of a vanilla autoencoder to incorporate relevant cardiovascular physiological signals; 2) Introduction of a novel loss function aimed at minimizing the I/O mapping of critical parameters such as left ventricular elastance, left ventricular contractility, aortic, mitral, and systemic vascular resistance into the latent space; 3) Development of a structured network capable of accepting external parameters to explore perturbed hemodynamic scenarios; 4) Presentation of a diagnostic model capable of classifying severity levels defined by parametric ranges from the existing literature pertaining to targeted cardiovascular diseases; and 5) The introduction of a novel approach for generating transient responses in cardiovascular hemodynamics, validated through *in vitro* and *in silico* testing.

II. THE FRAMEWORK OF THE ARTIFICIAL CARDIOLOGIST ASSITANT

The main objective of this research is to lay ground of a framework to analyze and predict the health condition of human CV system. In this section, we'll start with analogous reference model with lumped parameters of CVS. Then, preparation of the training and the test datasets are discussed with some explanations of cardiovascular degradation of some structural and functional impairment of left ventricular. At the same time an hMCL device is utilized to regenerate relevant physiological signals and parameters for validation purposes. We propose an autoencoder enhanced by some CV physiological parameters for a better CVS modeling. A cost function is derived to enable learning of both cardiovascular pressure-volume signals and some critical parameters playing roles in CVD diagnostics.

A. MODELLING CVS AND MORBIDITY

There have been numerous models at varying degrees of complexity showing the internal hemodynamics in the heart. For the purpose of left ventricular, that is considered to be the main driving part, study a reduce order lumped CVS model [5] has been taken as a reference model in this paper.

The analogous electrical circuit shown in Fig. 1 is written in state space as,

$$\dot{z} = A_c(t)z + B_c(t)p(z) \quad (1)$$

where $z = [P_{LV}(t) \, P_{LA}(t) \, P_{AP}(t) \, P_{AO}(t) \, Q_T(t)]^T$.

$$A_c(t) = \begin{bmatrix} \dfrac{\dot{C}_{LV}(t)}{C_{LV}} & 0 & 0 & 0 & 0 \\ 0 & \dfrac{-1}{R_{sys}C_{LA}} & \dfrac{1}{R_{sys}C_{LA}} & 0 & 0 \\ 0 & \dfrac{1}{R_{sys}C_x} & \dfrac{-1}{R_{sys}C_x} & 0 & \dfrac{1}{C_x} \\ 0 & 0 & 0 & 0 & \dfrac{-1}{C_{AO}} \\ 0 & 0 & \dfrac{-1}{L_x} & \dfrac{1}{L_x} & \dfrac{-R_x}{L_x} \end{bmatrix} \quad (2)$$

$$B_c(t) = \begin{bmatrix} \dfrac{1}{C_{LV}(t)} & \dfrac{-1}{C_{LV}(t)} \\ \dfrac{-1}{C_{LA}} & 0 \\ 0 & 0 \\ 0 & \dfrac{1}{C_{LA}} \\ 0 & 0 \end{bmatrix}$$

$$p(z) = \begin{bmatrix} \dfrac{1}{R_M} r(z_2 - z_1) \\ \dfrac{1}{R_{AO}} r(z_1 - z_4) \end{bmatrix} \quad (3)$$

With the ramp signal modeling the switching functionality of diodes,

$$r(\eta) = \begin{cases} \eta, & \text{if } \eta \geq 0 \\ \eta, & \text{if } \eta < 0 \end{cases} \quad (4)$$

The four phases, isovolumic relaxation and contraction, ejection, and filling, of the left ventricular response can now be represented by this model (1) using the lumped parameters.

The emulation of healthy and morbidity conditions is accomplished by reflecting structural deformations on the lumped aortic, mitral, systemic resistances and contractility of the left ventricular elastance in four severity levels, named S1 through S4. The parametric ranges of these conditions that are defined by our study are shown in Table 1.

In Table 1, CVS principal variables of a person in healthy and different stages of disease conditions are parameterized. In healthy condition, the E_{max} parameter range is shown to be between 1-5 mmHg/ml interval [26]. In our study, the proposed *in silico* model is tested between 1.4-2.5 mmHg/ml as in [5]. The ranges of abnormal cases of R_m and R_{sys} are selected according to the same study as well [5]. The R_{AO} values are taken from Iscan et al. studies [8] in which the time-varying aortic resistance is modeled in their study to represent the aortic regurgitation and stenosis cases. The last stage of the CVD demonstrates worst case condition (S4) for a given CV condition.

Therefore, the healthy condition is labeled as H_i when E_{max} value is taken from S_i^{th} column for $i = 1, 2, 3, 4$ and the remaining parameters kept at their nominal values as shown in column N in Table 1. The aortic stenosis (AS) severity level is labeled as AS_i when R_{AO} value is taken from the column
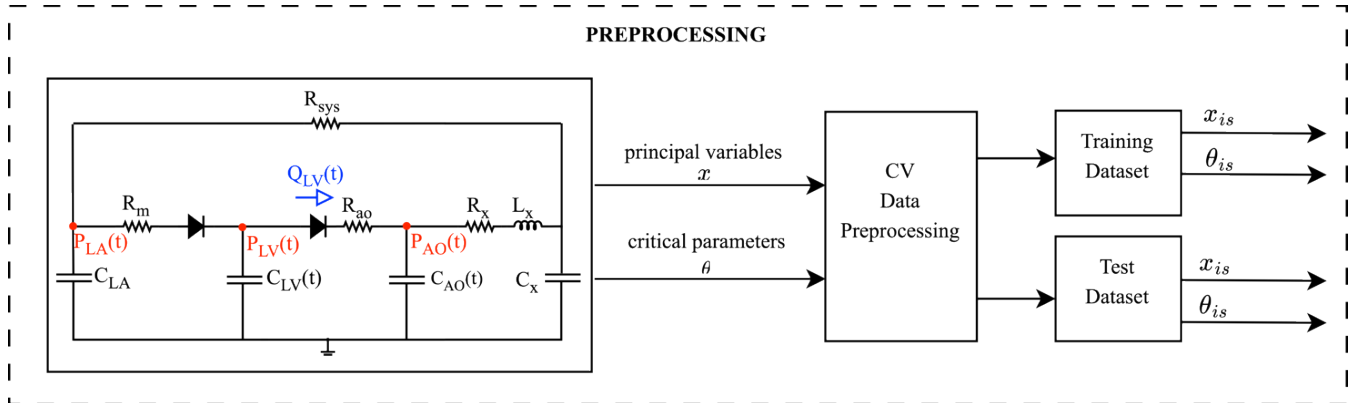
FIGURE 1. Dataset generation for CVS model development. In silico data are generated using Simaan's base model [5]. This in silico model can be conditioned to the specific CVS conditions such as aortic and mitral stenosis, systemic vascular change and variation in left ventricular contractility. The principal and critical variables are transferred into the data processing unit to split into training and test dataset.

TABLE 1. CV Health Condition Parameterization. The values of all variables primarily used for CVS conditions are provided in the table. The values of critical cardiovascular parameters were adjusted according to disease levels to create all in silico data. Parameter values were assigned based on the conformity of the hMCL in vitro tests with the reference in silico model.

Name		Value					Unit
		N	S1	S2	S3	S4	
R_{SYS}	Systemic Resistance	1.4	**1.7**	**2.0**	**2.3**	**2.5**	*mmHg.s/ml*
R_{AO}	Aortic Section Resistance	0.0005	**0.001**	**0.01**	**0.1**	**0.6**	*mmHg.s/ml*
R_M	Mitral Resistance	0.0003	**0.003**	**0.03**	**0.07**	**0.1**	*mmHg.s/ml*
E_{max}	Maximum End-Systole Elastance	2.5	**2.2**	**1.9**	**1.7**	**1.4**	*ml/mmHg*
R_C	Characteristic Resistance	0.04	0.04	0.04	0.04	0.04	*mmHg.s/ml*
C_{LA}	Left Atrium Compliance	4.4	4.4	4.4	4.4	4.4	*ml/mmHg*
C_{AO}	Aortic Compliance	0.08	0.08	0.08	0.08	0.08	*ml/mmHg*
C_S	Systemic Compliance	1.33	1.33	1.33	1.33	1.33	*ml/mmHg*
L_S	Inertance of blood in Aorta	0.0005	0.0005	0.0005	0.0005	0.0005	*ml/mmHg*

S_i while the others kept at nominal values. Similarly, for mitral stenosis (MS) and systemic resistance chance (SRC) conditions severity levels are labeled as MS_i and VSR_i by changing R_M and R_{SYS} from S_i^{th} column, respectively.

B. GENERATION OF CV PHYSIOLOGICAL DATASET FOR DEEP-LEARNING

In Fig. 1, the CV dataset generation process using reference CVS models is shown. To obtain the reference time series of the principal signals and critical parameters with the labeled healthy and disease conditions of the aortic and mitral stenosis, systemic vascular resistance change and maximum elastance variation, the model is run with different parameter. A representative latent space variables during the dataset generation is depicted in Fig. 2. These signals and the associated CV conditions are split into 30% test and 70% training datasets and stored during the preprocessing phase.

The training data is produced by using these resistances and maximum elastance values in which each of them is changed at different times and time responses of CVS are obtained to identify mitral and aortic stenosis, systemic vascular change and maximum elastance effect on cardiovascular parameters Each training set related to N, S1, S2, S3 and S4 for each condition is run within the period of 180 second with the sampling rate of 10Khz. After that, each condition is assigned to specific states defining the diseases type of CVS. After that, the normalization process is applied to the whole data to improve autoencoder results. Due to time dependency of CVS, the best beats are selected to represent the specific disease and its levels by using state variables which is assigned to both healthy and disease conditions. Then, the whole generated data is split into test and training one at the rate of %30 and %70, respectively. The total training and test data indicating disease and healthy conditions are depicted in Table 2.
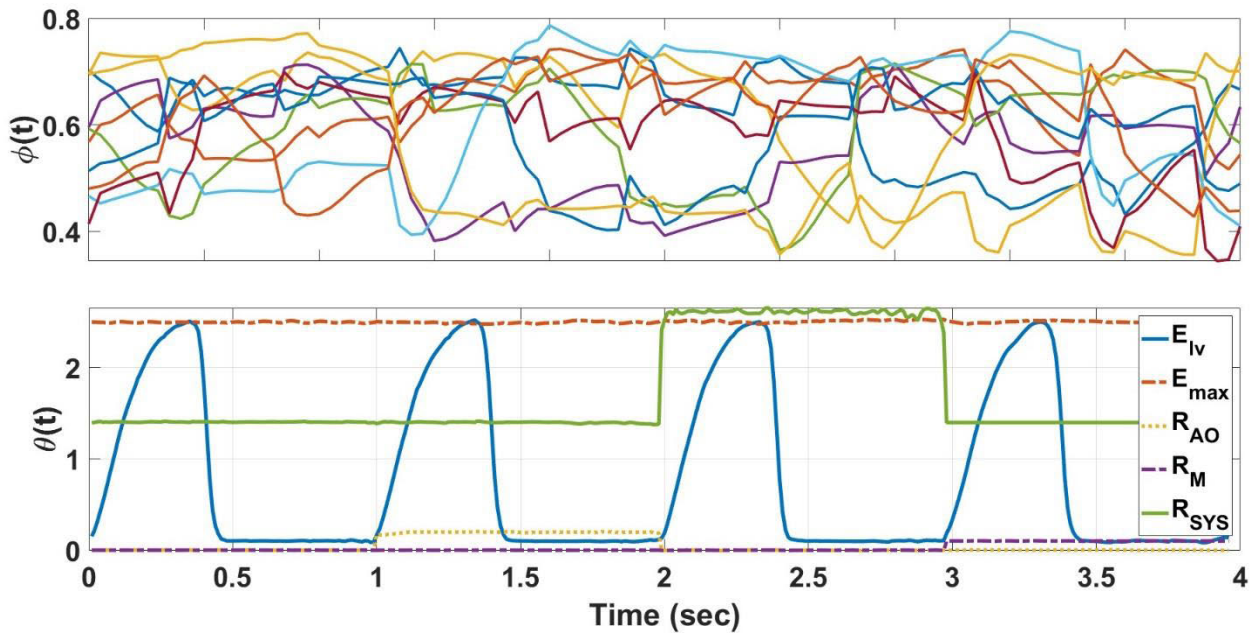
FIGURE 2. Latent variables during dataset generation. Each time-dependent variable consists of the total latent space in accordance with the CVS parameters. The key innovation is to create critical parameters of CVS using supervised learning to capture the history-dependent features of CVS.

TABLE 2. PCAE data slicing for training and validation.

All Level	In Silico (PV)	In Silico (CP)	In Vitro (PV)	In Vitro (CP)	Total
Training Data	11,500 beats	11,500 beats	-	-	**23,500 beats**
Test Data	5,000 beats	5,000 beats			**10,000 beats**
Validation Data	-	-	1,200 beats	1,200 beats	**2,400 beats**
Total	**16,500**	**16,500**	**1,200**	**1,200**	**35,400**

Validation Tests	In Vitro (PV)	In Vitro (CP)	Total
Healthy Test	398 beats	398 beats	**796 beats**
Mitral Stenosis Test	154 beats	154 beats	**308 beats**
Aortic Stenosis Test	227 beats	227 beats	**454 beats**
E_{max} Change Test	168 beats	168 beats	**336 beats**
Systemic-Vascular Change Test	253 beats	253 beats	**506 beats**

In Table 2, CV data is generated in beats, each representing one time history of heart circulation including complete systole and diastole phases. The hMCL device is set to a specific resistance and elastance values to simulate the targeted abnormalities.

Fig. 5 presents the hMCL configuration, encompassing LV, aorta, and LA tanks with liquid components in blue.

The LV tank features the mitral valve, transferring liquid from LA to LV during diastole, and the aortic valve, directing flow from LV to the aorta during systole. Three pipelines link tanks to adjustable resistances (R_M, R_A, R_V) for replicating pathophysiological states. To address LV's low-pressure nature, a balance tank ($Tank_1$) reduces gas pressure. A valve within the pipeline decreases pressure
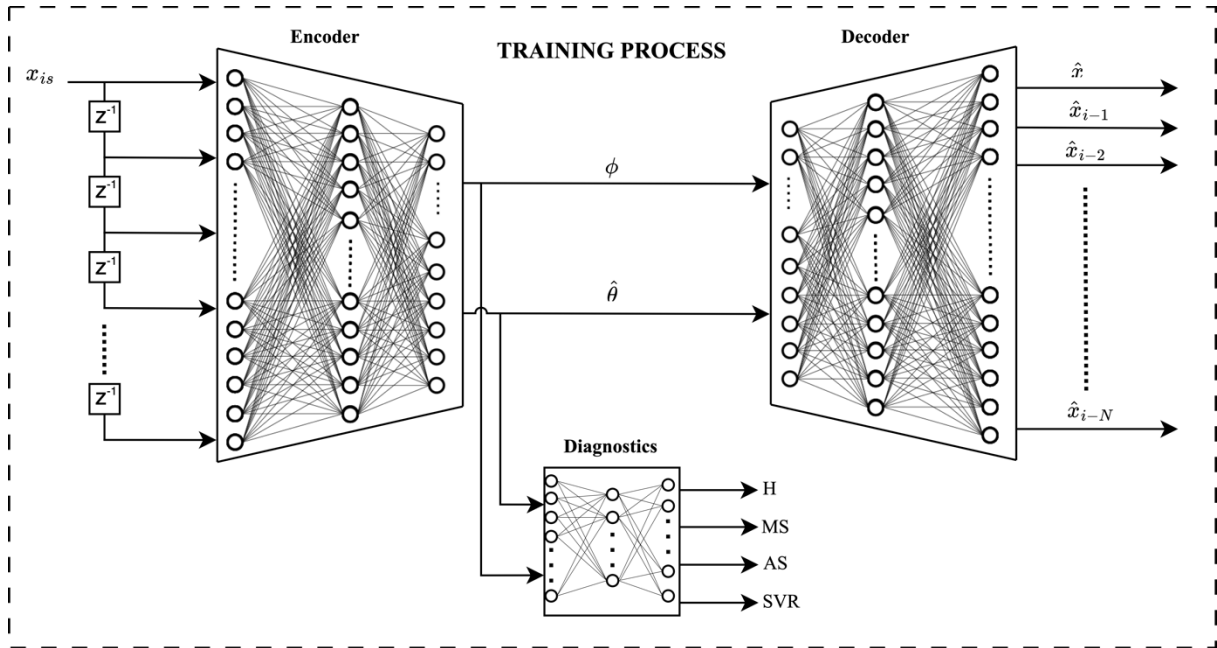
FIGURE 3. PCAE based CVD classification. Inputs are fed into the encoder with a time delay. Subsequently, outputs related to the latent space and critical parameters are generated between the encoder and decoder. In the decoder output, an attempt is made to reproduce the data provided in the input while also estimating critical cardiovascular parameters. For the diagnostic process, abnormal situation can be conditioned using the latent space and critical parameters that determine the system's response in the cardiovascular system.
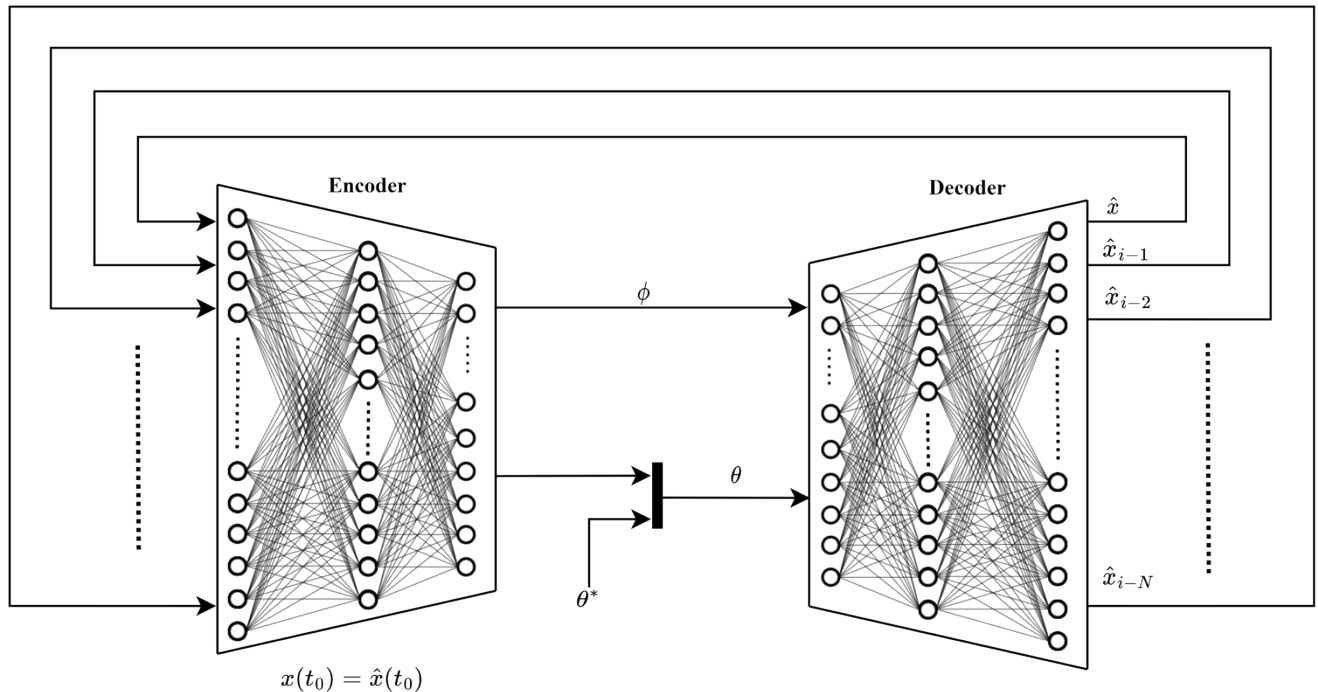
FIGURE 4. Closed loop PCAE operations. To test the performance of the presented PCAE, the connection of critical cardiovascular parameters can be severed, and external inputs can be fed. Moreover, the PCAE provided in the closed-loop response is designed to generate cardiovascular pressure-flow values. During this data generation, the output of the decoder is fed back to the input of the encoder. This feedback enables the feeding of additional critical cardiovascular parameters from external sources. Disease states, whether healthy or diseased, can be simulated using the presented PCAE by altering only the critical cardiovascular parameter values.

for ease of control. Proportional gas valves regulate gas inlet and outlet, responding to pressure differences between tanks. The system employs three valves (g_1, g_2, g_3) for

this purpose. The hMCL was assessed by modifying resistance values to replicate aortic stenosis and systemic abnormalities through orifice area adjustments, enabling time

response evaluation. Furthermore, diverse heart rate references were implemented to gauge cardiac output in relation to literature-documented physiological studies. The assessment of our proposed method encompasses evaluating hMCL capabilities, including variable stiffness, aortic and mitral stenosis, and changes in systemic resistance. Importantly, we demonstrate that existing hMCLs are incapable of simulating the FSM [36]. Our hMCL substantially enhances data diversity, yielding more precise physiological conditions. This experimental environment facilitates the simulation of diverse conditions that are unattainable through real tissue experiments or *in vivo* test. By rigorously replicating hMCL according to the values in Table 1 through numerous repeatable experiments, we broaden data diversity and encompass conditions untestable on real tissues.

The *in vitro* data is collected at 1 kHz on the platform developed by authors [10]. It is important to notice that only the *in silico* data is utilized during the training phase. Each of the training dataset is set to be 2,300 beats for each disease levels. The *in silico* tests are performed for 1,000 synthetic beats for each case. Additionally, hMCL measurements are only used to validate the proposed PCAE model.

Each feature vector related to the principal variables and the critical parameter values are normalized between 0 and 1 by using physiological maximum and minimum values (e.g., P_{LV} is ranged between 0 and 200 mmHg, etc.).

The training and testing features contain both principal variables $\boldsymbol{x} = (P_{lv}, P_{ao}, P_{la}, V_{lv}, Q_{lv})^T$ and critical parameter $\boldsymbol{\theta} = (E_{lv}, E_{max}, R_{ao}, R_m, R_{sys})^T$ sets in order to represent the targeted physiological properties related to normal and abnormal cases. The calculation of the critical parameter sets is done by using principal variables values at both *in silico* and *in vitro* experiments. In both experiments, normal and abnormal conditions are constructed by using Table 1 with the change of resistance and maximum elastance values. After that, the measurements of *in silico* and *in vitro* are achieved and assigned to specific cases for healthy and mitral, aortic stenosis, vascular resistance and elastance changes abnormalities.

C. THE PCAE ARCHITECTURE FOR CVS

The backbone of the proposed framework is Physiologically Conscious Auto-Encoder (PCAE) as shown in Fig. 3. The PCAE is constructed by feedforward neural networks (NN) mapping the recurrent principal variables input space to the latent space in the encoder block and then back to a prediction of the principal variables in the decoder block. Our innovative approach involves bifurcating the latent space, where information is condensed, which differs from standard autoencoder practices. Traditional auto-encoders capture essential features in this space to represent outputs. However, the CVS yields time-dependent results. To accommodate this, we introduce five physiologically conscious neurons within the latent space for supervised learning of critical parameters (resistance, capacitance). The standard autoencoder

structure is updated to include this augmented latent space. The remaining aspects of the vanilla autoencoder structure remain unaltered. These changes are applied to supervised learning through adjustments in the cost function and learning process. Consequently, our modified autoencoder can express time-dependent states within a unified framework. The latent space is modified by the cardiovascular parameters (CVP) that cannot be measured non-invasively, including aortic (AR), mitral (MR) and systemic (SR) resistances, end systole (Emax) and time-varying elastance of left ventricle (TV-LVE). The latent space vector is used for analysis and diagnostics of targeted CVD conditions with an additional feedforward NN, called diagnostics model. The CVS abnormalities considered are the left ventricular elastance (TV-LVE) deviation, mitral (MS) and aortic (AS) stenosis and vascular resistance change (VRC). Deep learning is achieved using *in silico* generated dataset based on the models given in [5]. The mathematical model is conditioned in both healthy and abnormal cases.

The PCAE is shown, processing the principal variable vector,

$$\boldsymbol{x} = (P_{lv}, P_{ao}, P_{la}, V_{lv}, Q_{lv})^T \tag{5}$$

with P_{lv}, P_{ao}, P_{la} the left ventricular, the aorta, the left atrium pressures, V_{lv}, Q_{lv} the left ventricular volume and flow rate, respectively. at the input stage and generates the latent space internal $\phi(k) \in \mathbb{R}^{N_1}$ and external $\theta(k) \in \mathbb{R}^{N_2}$ vectors at its output. The external $\theta(k)$ vector enables injection of external physiologically conscious into the PCAE. The decoder block maps the latent space back to predictions of the principal CV variables.

Since both principal variables and critical CVS parameters are time-dependent a recurrent autoencoder is used in our modeling. According to physiological information, the average heart rate in a healthy person is in the range of 60 to 120 bpm which means that the proposed method includes 1000 to 2000 samples collected at 1 kHz [27]. So, the input vector should be increased by using delay operation like

$$X = \begin{bmatrix} x_{is}(k) \\ x_{is}(k-1) \\ \vdots \\ x_{is}(k-N) \end{bmatrix} \tag{6}$$

with N picked large enough to form a window to enable learning in time series.

After completing the preprocessing and data collection phase extended PCAE input vector X and focused parameters θ_{is} are made available for physiologically conscious learning process. The input X is predicted by autoencoder, θ_{is} injected into the loss function to steer some of the latent space neurons to select physiological parameters simultaneously.

Let error vectors be,

$$\boldsymbol{e_x} = X - \hat{X}, \quad \boldsymbol{e_\theta} = \theta_{is} - \hat{\theta} \tag{7}$$

with e_x and e_θ the autoencoder prediction and critical parameter error vectors, respectively. In this study, we target critical

parameters of interest.

$$\hat{\theta} = \left[\hat{E}_{LV}, \ \hat{E}_{MAX}, \ \hat{R}_{AO}, \ \hat{R}_{SYS}, \ \hat{R}_M \right]^T \qquad (8)$$

to be estimated within the latent space.

The proposed augmented autoencoder model consists of two phases: encoder and decoder sections. The encoder maps the input vector to another one by using (9)-(11):

$$z^{(1)} = h^{(1)} \left(W^{(1)} X + b^{(1)} \right) \qquad (9)$$

$$z^{(2)} = h^{(2)} \left(W^{(2)} z^{(1)} + b^{(2)} \right) \qquad (10)$$

$$\gamma = h^{(3)} \left(W^{(3)} z^{(2)} + b^{(3)} \right) \triangleq f(X, \Theta_e) \qquad (11)$$

where the superscript indicates the layer number, $W^{(i)}$ is the weight matrices and $b^{(i)}$ is the bias vector, $h^{(i)}$ is the activation function of ith layer, Θ_e all learnable encoder parameters. The encoder is constructed by a three hidden layer MLP. The encoder output layer is split into internal ϕ and external $\hat{\theta}$ fields.

$$\gamma = \left[\phi^T \ \hat{\theta}^T \right]^T \qquad (12)$$

where $\phi^T = [\phi_1 \phi_2 \ldots \phi_m], \hat{\theta}^T = [\hat{E}_{LV} \ \hat{E}_{max} \ \hat{R}_{AO} \ \hat{R}_{SYS} \ \hat{R}_M]$. The following decoder block is organized as,

$$z^{(4)} = h^{(4)} \left(W^{4)} \gamma + b^{(4)} \right) \qquad (13)$$

$$z^{(5)} = h^{(5)} \left(W^{(5)} z^{(4)} + b^{(5)} \right) \qquad (14)$$

$$\hat{X} = h^{(6)} \left(W^{(6)} z^{(5)} + b^{(6)} \right) \triangleq g(\gamma, \Theta_d) = g \circ f(X, \Theta) \qquad (15)$$

where $\hat{X}$ is the predicted principal variables, $z^{(i)}$ hidden layer output, $W^{(i)}$ and $b^{(i)}$ are i^{th} layer tunable weight and bias matrices, Θ_d all learnable decoder parameters and $\Theta = \{\Theta_e, \Theta_d\}$.

The cost function to train the autoencoder while guiding a subset of the latent space is defined as

$$J = \alpha_1 \frac{1}{N} \sum_{n=1}^{N} e_x^T e_x + \alpha_2 \frac{1}{N} \sum_{n=1}^{N} e_\theta^T e_\theta$$
$$+ \lambda \Omega_{weights} + \beta \Omega_{sparsity} \qquad (16)$$

where N is the total number of training samples, α_1 and α_2 are the weights of variable prediction and parameter estimation processes, λ is the L2 regularization term and β is the sparsity regularization term, respectively. For the L2 regularization, we have,

$$\Omega_{weights} = \frac{1}{2} \sum_{l=1}^{L} \sum_{j=1}^{n_l} \sum_{i=1}^{k_l} \left(w_{ji}^{(l)} \right)^2 \qquad (17)$$

with L, n_l, n_k the number of hidden layers, the number of neurons in the layer l, and the following layer, respectively. For the sparsity rate, the Kullback-Leibler divergence formula is used as in [28]:

$$\Omega_{sparsity} = \sum_{i=1}^{D^{(1,\ldots,6)}} \rho \log \left(\frac{\rho}{\hat{\rho}} \right) + (1-\rho) \log \left(\frac{1-\rho}{1-\hat{\rho}} \right) \qquad (18)$$

where ρ is sparsity proportion rate value and $\hat{\rho}$ is the estimated average output function value. The $\hat{\rho}$ is calculated as

$$\hat{\rho}_i^{(l)} = \frac{1}{N} \sum_{j=1}^{N} z_i^{(l)} z_j^{(l-1)} \qquad (19)$$

The cost function given in (16) is optimized using the scaled conjugate gradient method [9]. The total error value is also calculated by using the mean square error.

D. DIAGNOSTICS MODEL

The proposed framework includes another deepnet diagnostics model to predict and classify the CV health conditions including the severity level of abnormalities for the trained diseases. A multilayer perceptron model with a softmax layer is utilized to achieve these tasks for 16 classes of abnormalities which contains 4 healthy conditions with respect to critical parameter sets of input variables.

The diagnostics model input is taken from the latent space of PCAE,

$$\gamma = \left[\phi_1 \phi_2 \ldots \phi_m \ \hat{E}_{LV} \ \hat{E}_{max} \ \hat{R}_{AO} \ \hat{R}_{SYS} \ \hat{R}_M \right]^T \qquad (20)$$

Its output is the healthy and disease condition levels of 16 classes. The output layer's softmax activation function is [29], then

$$\sigma(z)_i = \frac{e^{z_i}}{\sum_{j=1}^{K=16} e^{z_j}} \qquad (21)$$

with $\sigma(\mathbf{z})_i$ the probability of i. The hidden layers use sigmoid activation functions, and the cross-entropy function is performed to train the network.

Each of the class probabilities are obtained from (20), then, the class which has maximum probability is assigned to 1 to represent the stage of both healthy and diseases conditions.

E. USE OF PCAE FOR CVD TREATMENT

Once the PCAE is trained for the targeted abnormalities and healthy conditions, the critical parameters may be externally injected into the framework to observe their effects on the CVS principal variables. This mechanism enables an expert physician to tailor some treatment strategies targeting those critical parameters and analyze the CVS response. Total representation of closed loop PCAE is given in Fig. 4.

After the training process, autoencoder output is feedback to its input and the network is put in a cyclic condition. At this stage the latent space parameter vector element(s) may be switched to a desired parameter $\theta^*(t)$. The cyclic autoencoder output converges to a different regimen that is correlated to the corresponding principal variable state, hence the effect of changing some of the critical parameters on CVS are observed in detail by a cardiologist.

III. ILLUSTRATIONS

To demonstrate the capabilities of the proposed framework, we have first showed the training and test performances PCAE model driven by *in silico* healthy, aortic and
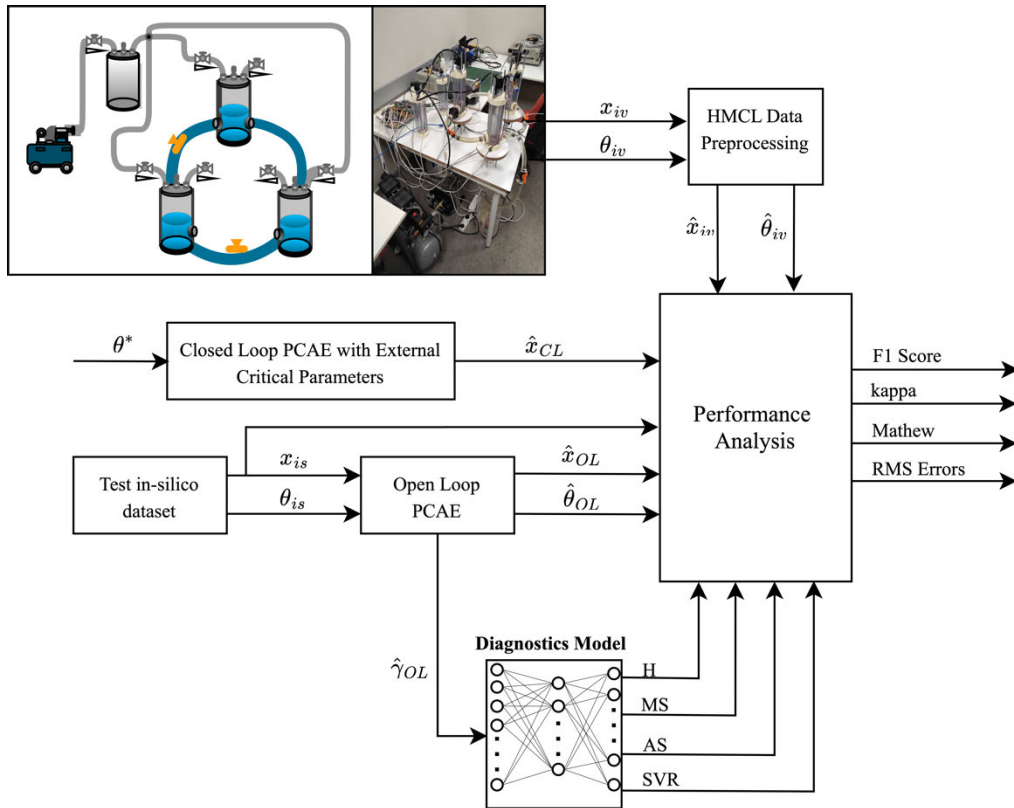
FIGURE 5. Validation process of the proposed PCAE algorithm. All reference data were generated using hMCL. In the tests, in silico, open-loop, and closed-loop PCAE data were compared for performance analysis. Additionally, disease levels for the diagnostic model were compared in percentage units, and measurements were validated by generating F1 scores, Kappa, and Matthew's correlation coefficients. Validation was completed using RMS error values for the comparison of physiological signals.

mitral stenosis, and systemic vascular resistance deviation case datasets. Then, the PCAE model is validated on *in vitro* tests. Then, the artificial cardiac assist model's performance is shown. Finally, we have shown PCAE CV model response to some select critical parameter changes, including E_{max}, R_{ao}, R_{sym}. Fig. 5 demonstrates the overall performance analysis process applied for model assessment. All these simulations resulted in the principal variables, critical parameters consistent with the literature and %94 F1 score accurately classify the selected diseases.

In Fig. 5, *in silico* test dataset is generated $x_{is} = \{P_{lv}, P_{ao}, P_{la}, V_{lv}, Q_{lv}\}_{is}$ and critical parameters $\theta_{is} = \{E_{lv}, E_{max}, R_{ao}, R_m, R_{sys}\}_{is}$ using (1) while the *in vitro* tests are conducted to produce the same physiological dataset x_{iv} and θ_{iv}. The trained PCAE driven by x_{is} predicts CV variables $\hat{x}_{OL}$ and parameters $\hat{\theta}_{OL}$. The processed *in vitro* test outputs $\hat{x}_{iv}$ and $\hat{\theta}_{iv}$ are compared to model outputs in the performance analysis. The latent space vector $\hat{\gamma}_{OL}$ is utilized by the diagnostics model for the CVD classification with the outputs of four stages of each Healthy (H), Mitral Stenosis (MS), Aortic Stenosis (AS) and Systemic Vascular Resistance (SVR) change conditions.

A. PCAE MODELING SIMULATIONS

The hyper-parameter optimization was accomplished by changing their values which was given in Table 3. In Table 3, there were five basic parameters to optimize the proposed augmented autoencoder in terms of HLS-S, EF, DF, λ, β, and ρ. Firstly, EF and DF were iterated by changing its activation function resulting the best combination with "logistic sigmoid" and "pure linear" one. After that, the symmetric hidden layer size and neuron numbers were improved until the best performance were found out in which it was reached at "200-120-10" and "15-120-200" for encoder and decoder, respectively. Notice that the decoder input was increased up to 15 by feeding critical parameter sets. The best performance was indicated as italic and bold line in Table 3 which had 3.436e-4 general mean square error. On the other hand, the best performance was changed in evaluation of critical parameter sets due to fact that the cost function parameters of the error were set to be ($\alpha_1 = 10$, $\alpha_2 = 1$).

After experimenting with some of the hyper-parameters, we have reached satisfactory results when the encoder hidden layers of 200-120-15, and $\lambda = $1e-10, $\beta = $1e-12, $\rho = $1e-5, $\alpha_1 = 10, \alpha_2 = 1$ are selected.

TABLE 3. Auto-encoder hyper parameterization MSE results. All hyperparameter variations were evaluated sequentially based on their performance. With each change, the best parameter was identified, and the next Parameter adjustment process was completed.

EF	DF	HLS-S	λ	β	ρ	G-MSE	P_{LV}-MSE	P_{AO}-MSE	P_{LA}-MSE	V_{LV}-MSE	Q_{LV}-MSE
logsig	logsig	15 10 5	1e-6	1e-4	1e-1	3.644e-1	1.341e-2	4.633e-1	3.176e-2	6.846e-2	5.396e-1
logsig	satlin	15 10 5	1e-6	1e-4	1e-1	1.242e-1	4.615e-2	2.51e-2	9.492e-2	4.711e-2	1.372e-1
logsig	*purelin*	*15 10 5*	*1e-6*	*1e-4*	*1e-1*	*3.869e-3*	4.161e-3	1.017e-3	1.027e-2	2.682e-3	3.297e-3
logsig	purelin	50 40 10	1e-6	1e-4	1e-1	6.460e-4	3.983e-4	5.401e-4	3.732e-4	4.313e-4	1.752e-3
logsig	purelin	100 60 10	1e-6	1e-4	1e-1	6.476e-4	4.941e-4	6.012e-4	3.342e-4	5.808e-4	1.430e-3
logsig	purelin	*200 120 10*	1e-6	1e-4	1e-1	*6.448e-4*	4.929e-4	6.063e-4	3.497e-4	6.135e-4	1.500e-3
logsig	purelin	50 40 20	1e-6	1e-4	1e-1	6.462e-4	4.078e-4	5.526e-4	3.743e-4	4.419e-4	1.564e-3
logsig	purelin	100 60 20	1e-6	1e-4	1e-1	6.478e-4	4.695e-4	5.867e-4	3.724e-4	6.017e-4	1.016e-3
logsig	purelin	200 120 20	1e-6	1e-4	1e-1	6.456e-4	3.918e-4	5.598e-4	3.216e-4	5.794e-4	1.143e-3
logsig	purelin	50 40 30	1e-6	1e-4	1e-1	6.465e-4	4.278e-4	5.791e-4	3.764e-4	5.203e-4	1.305e-3
logsig	purelin	100 60 30	1e-6	1e-4	1e-1	6.479e-4	4.731e-4	5.848e-4	3.326e-4	5.441e-4	1.539e-3
logsig	purelin	200 120 30	1e-6	1e-4	1e-1	6.454e-4	3.935e-4	5.701e-4	3.461e-4	5.601e-4	1.637e-3
logsig	purelin	200 120 10	1e-8	1e-4	1e-1	3.504e-4	2.766e-4	4.376e-4	2.717e-4	3.951e-4	6.409e-4
logsig	purelin	200 120 10	*1e-10*	1e-4	1e-1	*3.486e-4*	1.792e-4	4.509e-4	1.694e-4	4.154e-4	5.642e-4
logsig	purelin	200 120 10	1e-10	1e-8	1e-1	3.482e-4	2.185e-4	4.589e-4	2.032e-4	3.975e-4	5.679e-4
logsig	purelin	200 120 10	1e-10	*1e-12*	1e-1	*3.449e-4*	1.978e-4	4.394e-4	2.140e-4	3.869e-4	6.166e-4
logsig	purelin	200 120 10	1e-10	1e-15	1e-1	3.464e-4	1.548e-4	4.735e-4	2.408e-4	3.959e-4	5.794e-4
logsig	purelin	200 120 10	1e-10	1e-12	1e-3	3.447e-4	2.904e-4	4.595e-4	2.492e-4	3.869e-4	6.170e-4
logsig	*purelin*	*200 120 10*	*1e-10*	*1e-12*	*1e-5*	*3.436e-4*	*2.407e-4*	*4.542e-4*	*2.238e-4*	*3.844e-4*	*5.849e-4*
logsig	purelin	200 120 10	1e-10	1e-12	1e-7	3.460e-4	1.704e-4	4.873e-4	2.357e-4	4.206e-4	6.132e-4

EF	DF	HLS-S	λ	β	ρ	G-MSE	E_{LV}-MSE	E_{MAX}-MSE	R_{AO}-MSE	R_{M}-MSE	R_{SYS}-MSE
logsig	purelin	200 120 10	1e-10	1e-4	1e-1	1.045e-3	1.763e-3	1.489e-3	1.132e-3	1.048e-4	7.340e-4
logsig	purelin	200 120 10	1e-10	1e-12	1e-1	8.622e-4	1.769e-3	5.607e-4	9.978e-4	9.313e-5	8.902e-4
logsig	purelin	200 120 10	1e-10	1e-15	1e-1	8.527e-4	1.764e-3	8.135e-4	8.981e-4	9.472e-5	6.935e-4
logsig	purelin	200 120 10	1e-10	1e-12	1e-5	7.330e-4	1.763e-3	5.777e-4	7.000e-4	1.080e-4	5.166e-4
logsig	*purelin*	*200 120 10*	*1e-10*	*1e-12*	*1e-7*	*7.102e-4*	*1.772e-3*	*5.953e-4*	*5.540e-4*	*1.638e-4*	*4.654e-4*

HLS-S: Hidden Layer Structure Symmetry, *EF*: Encoder Function, *DF*: Decoder Function, λ: L2 Weight Regularization Rate, β: Sparsity Regularization Rate, ρ: Sparsity Proportion Rate, *G-MSE*: General Mean Square Error.

The trained PCAE is able to match the *in silico* data very closely for all of Heathy, Aortic Stenosis (AS), Systemic resistance (SYS), Mitral Stenosis (MS) cases as shown in the first columns for the principal variables in Fig. 6 and for the critical parameters in Fig. 7. When the same CVS conditions are generated *in vitro* tests PCAE responses are shown in the second columns in Fig. 6 for the principal variables and in Fig. 7 for the critical parameters. Although the physical limitations of hMCL device used showing some lag and noisy response for E_{lv}, Q_{LV}, E_{max} the remaining variables and parameters have resulted in anticipated signals.

In terms of the diseases cases, AS affects only the left ventricular pressure, the volume, and the flow rate at both *in vitro* and *in silico* data are in accordance with the physiological findings [25]. Vascular systemic resistance increment pulled up aortic pressure to 150 mmHg but did not affect the $Q_{LV}(t)$ value in all cases. In the mitral stenosis case, all of the

pressures and volume values except $P_{LA}(t)$ are decreased in accordance with the physiological data [30].

Especially for $Q_{LV}(t)$ in diastole phase, highly sensitivity to transfer blood into the left ventricle chamber can be seen.

The other parameters $R_{ao}(t)$, $R_M(t)$ and $R_{SYS}(t)$ have perfectly converged to their reference physiological values [10], [12], [30], [31].

Notice that even though the model is trained on the *in silico* tests, overall performance of the PCAE is acceptably well when driven by the *in vitro* tests for all cases studied.

The classification performance of each class is shown in the confusion matrix depicted in Fig. 8. Although the overall performance of 94.76% correct classification is found to be satisfactory, it suggests even better results by paying attention to the following observations. The model's confusion between H-I and H-II as well as AS-I and AS-II is likely to be due to the assumptions made in Table 1.
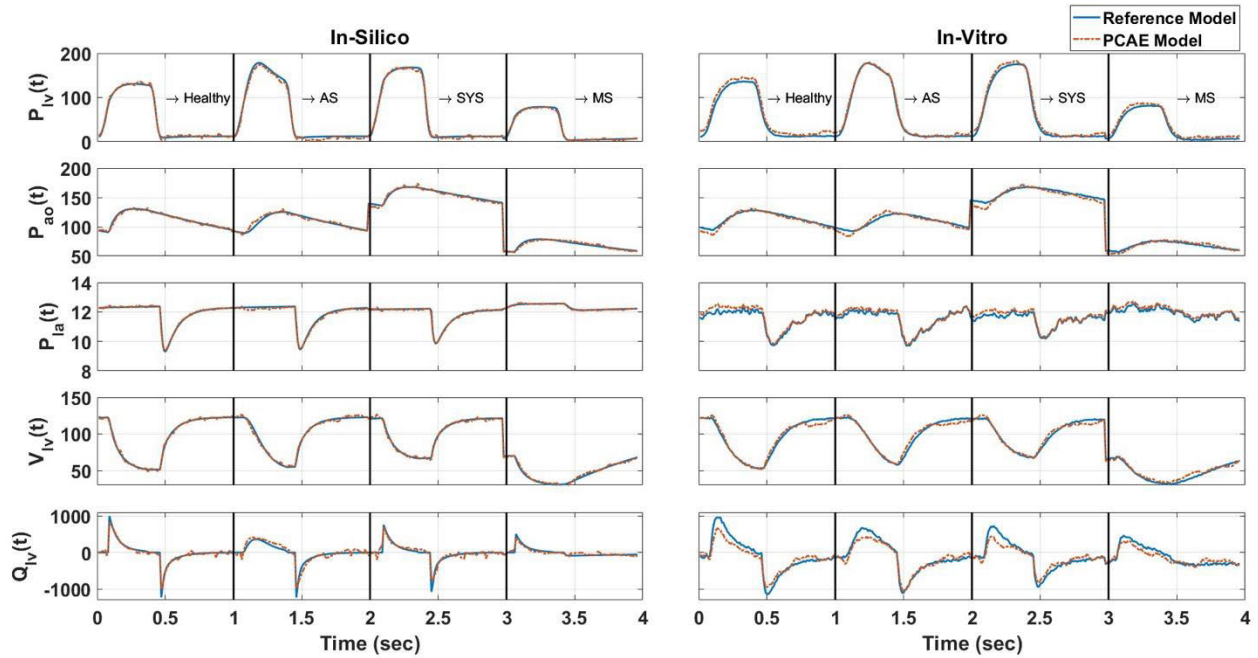
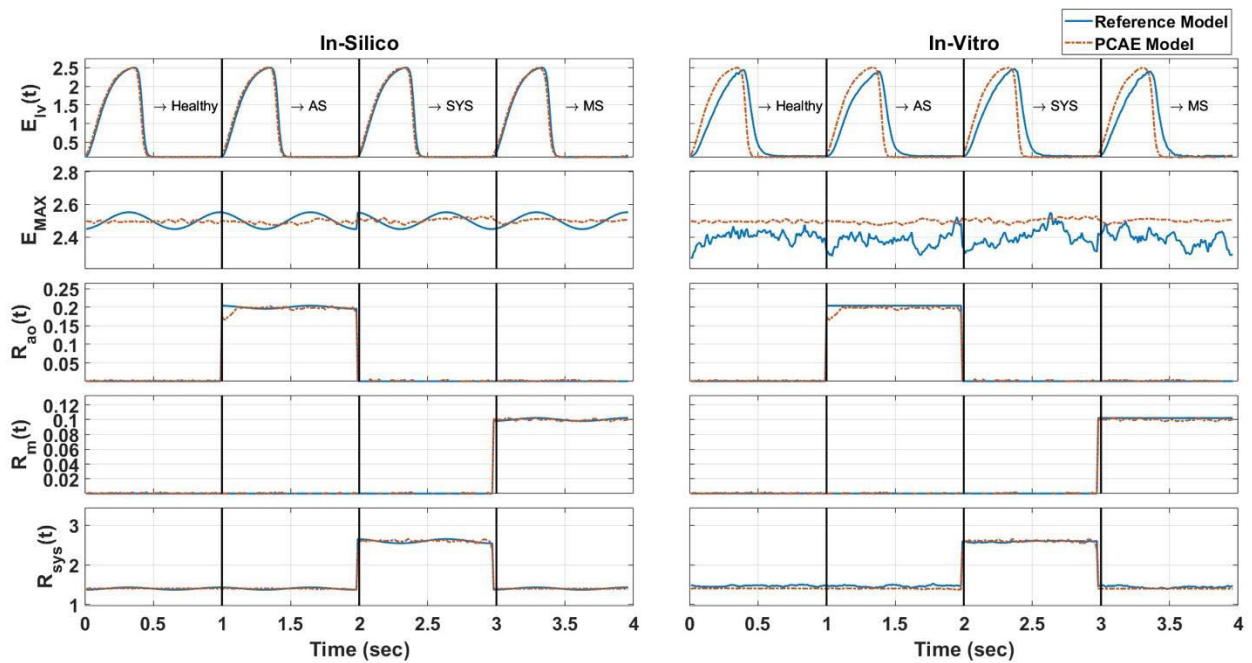**FIGURE 6.** PCAE principal variables responses to In silico model and in vitro device [10].

FIGURE 7. PCAE critical parameter responses to in silico model and in vitro device [10].

Especially for H-I and H-II, the acceptable E_{MAX} and P_{LV} values were increased in the healthy physiological range while V_{LV} was kept constant in accordance with the frank-starling law [32]. Similar observation has been noticed for AS-I and AS-II case, where the V_{LV} is kept constant through the time response.

In order to show a statistical performance of the proposed diagnostics model, F1 score together with the Matthews Correlation Coefficient (MCC) [33] and the kappa statistics [34] given in Table 4. MCC is added to take into account of the imbalance between *in silico* and *in vitro* tests and the kappa statistics is included to illustrate interrater reliability.

FIGURE 8. The confusion matrix of the CVS diagnostics model classification.

TABLE 4. The classification results of CVS data.

| Classes | Overall F1: 94.76%, Matthews Correlation: 94.32% | | |
	MCC	Kappa	F1 Score
H Stage I	86.87%	87.72%	87.68%
H Stage II	87.82%	87.61%	88.58%
H Stage III	99.36%	87.47%	99.40%
H Stage IV	100.00%	87.49%	100.00%
AS Stage I	86.30%	87.87%	87.12%
AS Stage II	87.69%	87.32%	88.45%
AS Stage III	97.21%	87.59%	97.38%
AS Stage IV	99.37%	87.42%	99.40%
VSR Stage I	91.89%	87.56%	92.40%
VSR Stage II	97.22%	87.54%	97.39%
VSR Stage III	91.60%	87.36%	92.13%
VSR Stage IV	94.62%	87.66%	94.95%
MS Stage I	94.27%	87.46%	94.63%
MS Stage II	95.50%	87.60%	95.77%
MS Stage III	99.57%	87.50%	99.60%
MS Stage IV	99.79%	87.52%	99.80%

Thus, Table 4 indicates that the use of *in silico* and *in vitro* tests on CVD conditions results in a reliable classification by the proposed model.

B. EXCITATION OF PCAE BY CRITICAL PARAMETERS

The PCAE in the closed-loop operation produces cyclic CVS variable signals consistent with the literature. When a critical
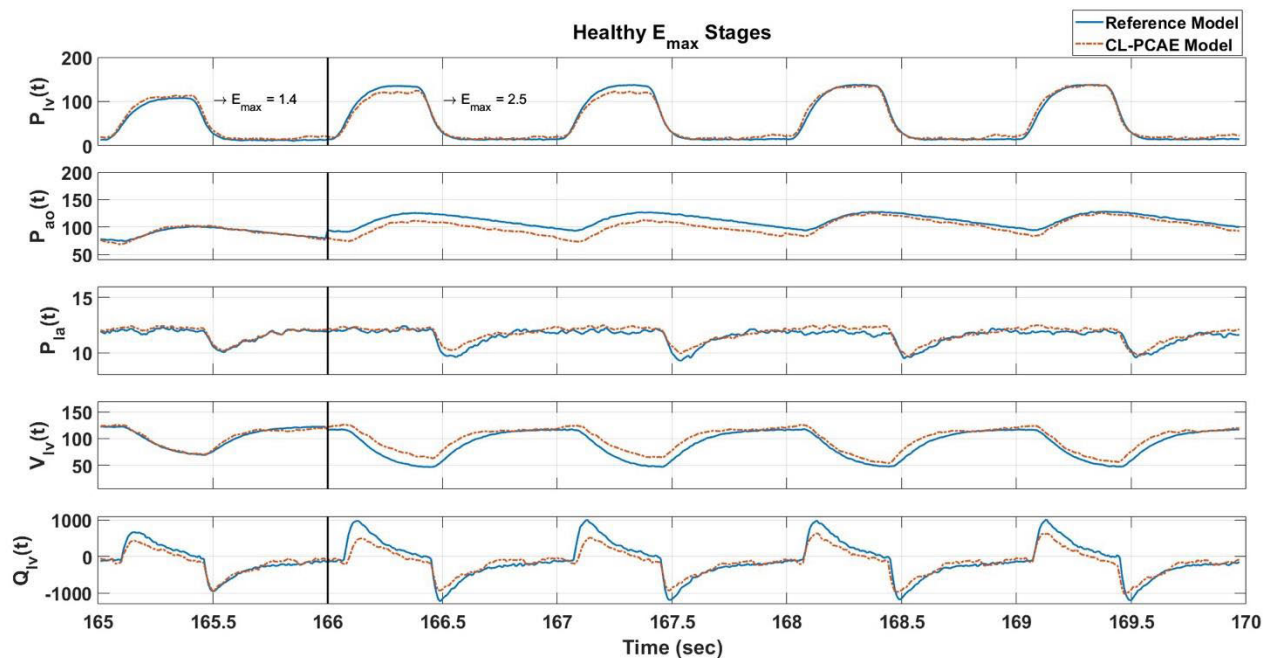
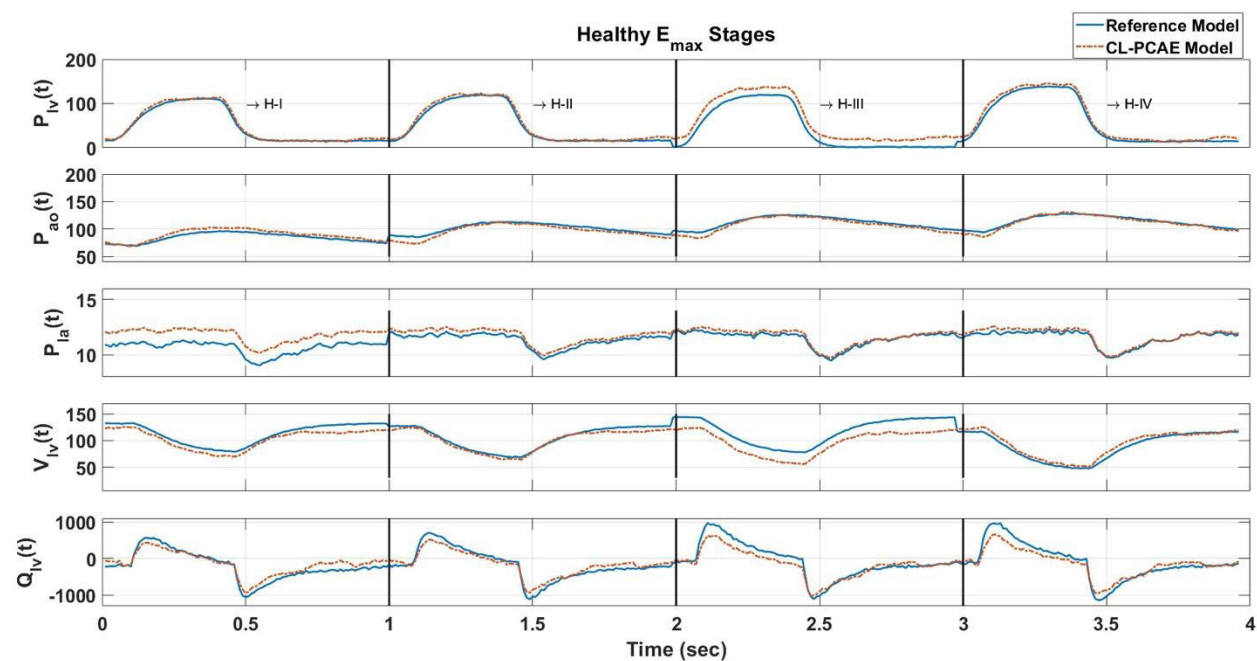**FIGURE 9.** Transient response of CVS PVs to externally triggered Emax.

FIGURE 10. Healthy case of the CL-PCAE results.

parameter defined within the latent space is deviated from its current condition to change the severity level, we observe that the model outputs, the principal variables, converge to the new state condition observed in *in vitro* tests conducted by the hMCL device. Fig. 9 shows the *in vitro* data as reference with H-IV level triggered at 166 s when $\theta_2^* = E_{max}^*$ value is changed to the nominal condition of 2.5 ml/mmHg.

The figure demonstrates the output transition of the PCAE model that is converging to the reference signals after a couple of cardiac cycles.

We have, then, carried out similar experiments for the other parameters in different morbidity settings. Fig. 10 depicts the PVs in H-I through H-IV conditions at the steady state.
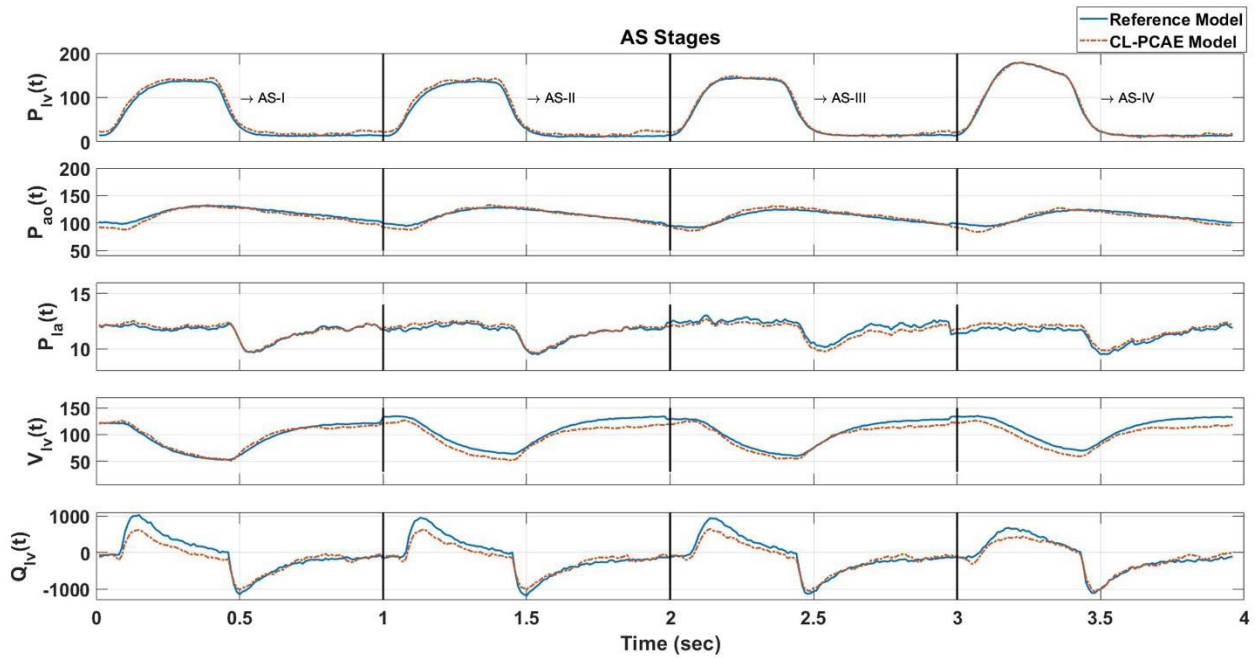
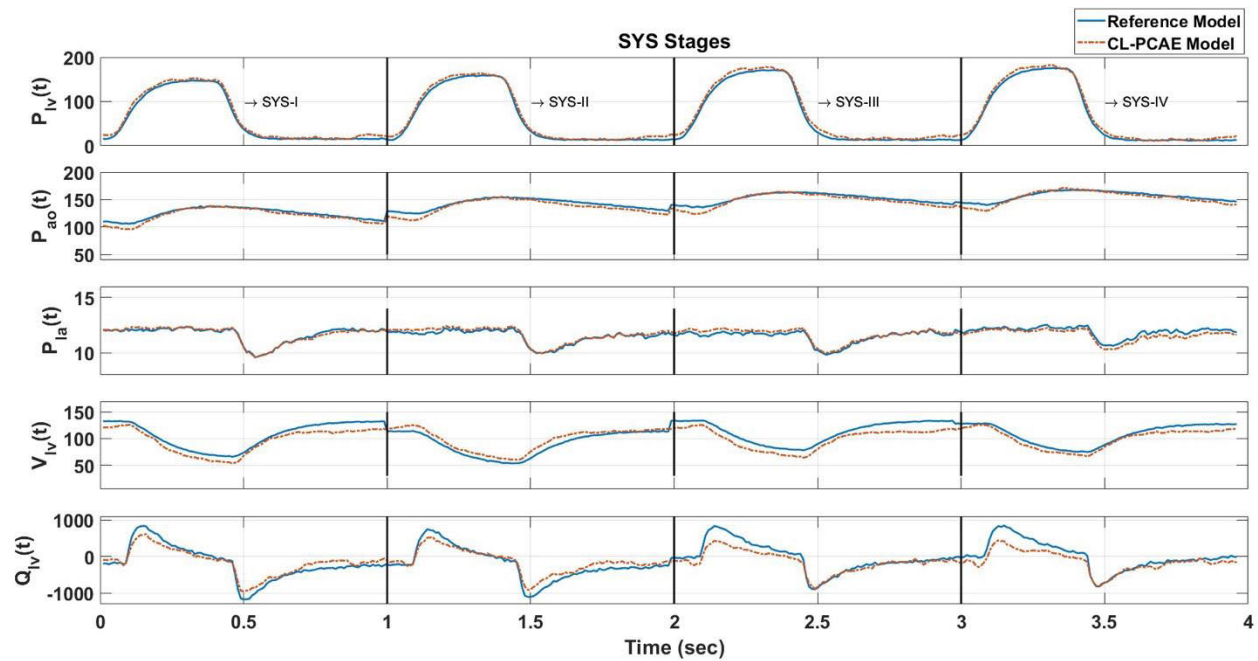**FIGURE 11.** Aortic stenosis case of the CL-PCAE results.

FIGURE 12. Systemic resistance change case of the CL-PCAE results.

The aortic stenosis levels, AS-I – AS-IV, are emulated in the PCAE model by adjusting $\theta_3^* = R_{AO}^*$ and validated by hMCL responses. The steady-state cardiac cycle waveforms for each case are illustrated in Fig. 11.

It noteworthy to mention that only $P_{lv}(t)$ values are increased that is in accordance with the literature [8]. Besides, the left ventricular volume was decreased in time while $P_{la}(t)$

was not changed at all stages. It was considered another important property for modelling aortic stenosis that is in consistent with physiological CVS dynamic.

For systemic resistance changes, Fig. 12 demonstrated the results of CL-PCAE outputs.

The PCAE model in closed loop possessed perfectly matched results for the whole pressures. The increment on

TABLE 5. The comparison of estimation of CVS parameters.

	(%)	R_{SYS}	R_M	E_{MAX}	P_{LV}	V_{LV}
Physiological Ventricle	Dabiri et al. [23]	-	-	-	0.939 ±0.067	0.923 ±0.050
	Bonnemain et al. [20]	-	-	1.10 ±0.88	-	-
	Laubsher et al. [21]	-	-	0.37 ±NA	-	-
	Bikia et al. [26]	-	-	6.4 ±5.00	-	-
	Regazzoni et al. [35]	-	-	-	**0.51** ±NA	0.22 ±NA
	Yang et al. [24]	0.3 ±NA	-0.54 ±NA	-0.29 ±NA	-	-
	Rapp et al. [25]	1.3 ±0.43	-	-	-	-
	Pawar et al. [22]	3.4 ±NA	-	1.53 ±NA	4.67 ±1.06	-
	The PCAE (in silico)	**-0.09** ±0.01	-0.41 ±0.57	**0.24** ±2.52	-0.58 ±1.36	**-0.04** ±1.57
	The PCAE (in vitro)	4.65 ±1.65	**-0.32** ±0.57	-6.07 ±4.03	-4.34 ±1.86	-0.49 ±4.16

the aortic pressure shown in Fig. 12 is also in accordance with hMCL measurements. These responses perfectly matched the hMCL measurements as well as physiological response of systemic resistance change [10].

We have encountered eight different studies within our scope, and we compare our results from the proposed framework on CVS signals estimation to those reported in theirs. The error signal mean (%) and STD values are listed in Table 5. Dabiri et al. establishes a machine learning technique to estimate the real-time left ventricular response using the finite element methods to train XGboost and Cubist network structure [23]. Their models yield high mean but low STD in errors in the left ventricular pressure and volume 0.939±0.067% and 0.923±0.050%. Regazzoni et al. worked on the left ventricular model with electrical and 3D modeling techniques to find proper outputs for the pressure and the volume [35]. The articles focused only on estimation of the left ventricle end-systolic elastance value [20], [21], [26] using CNN and DNN models are employed on both LVAD designs and real patients. On the other hand, Yang et al. suggested an inverse problem for the seven parameters of the same model of ours together with E_{max} and E_{min} estimation based on nonlinear optimization assuming using the systemic arterial pressure [24]. The study given in [25] focuses only on vascular resistance change R_{sys} while [22] extends it to the contractility change and the left ventricular pressure. Both are built on EKF based estimation of the CVS parameters using LVAD device-based measurements. The proposed PCAE model trained on Simaan et al. model results

in very competitive estimations over the critical parameters as summarized in the table.

IV. DISCUSSION

The presented study employs an autoencoder-based methodology, which is integrated into physiological consciousness framework. This innovative approach enables the modeling not only of pressure-flow dynamics but also the time-dependent characteristics of CVS, encompassing resistance and capacitance values. Specific CV conditions are selected, building upon our prior work, where we successfully simulated diseases relevant to the hMCL through stenosis and stiffness alterations [10]. To assess the method's accuracy without in-vivo data, experiments were conducted under conditions well-matched to hMCL capabilities. This narrowing of the focus is essential for clinical applicability, ensuring alignment with the range of cardiovascular conditions realistically emulated by the present hMCL. The widespread utility of this algorithm for diverse populations and various cardiovascular diseases, as emphasized in the review, is of paramount importance. Our method was rigorously trained using *in silico* data via the autoencoder structure and subsequently validated with *in vitro* data. This approach serves to illustrate that the algorithm's overall performance remains robust even when *in vitro* data is excluded from the training process. Thus, our objective is to demonstrate that by effectively learning critical parameters, such as resistance and capacitance, across a spectrum of cardiovascular diseases, the model can accurately reproduce the cardiovascular

system's response across a broad range of clinical scenarios.

The present study deliberately employs *in silico* data for comprehensive training of the proposed method, as highlighted in Table 2, with a deliberate exclusion of *in vitro* data during the training phase. This decision is made to rigorously evaluate the algorithm's performance when tested with real, *in vitro* data. In our *in vitro* investigations, the existing hMCL system adeptly models stenosis and variable stiffness values, successfully simulating the Frank-Starling mechanism [9]. Furthermore, its capacity to accommodate nonlinear fluid flow characteristics, account for pressure drops, and adapt to diverse resistance values positions hMCL to yield results closely aligning with real patient outcomes in *in vitro* studies. Importantly, hMCL's utilization can effectively simulate a wide spectrum of CV conditions, often surpassing real tissue simulations in accuracy. Additionally, investigating mitral and aortic stenosis conditions in actual patients poses formidable challenges, necessitating invasive sensor interventions that directly perturb CV hemodynamics, potentially yielding results that diverge from authentic clinical observations.

The presented methodology offers significant advantages by enabling the acquisition of diverse cardiovascular data using a single, efficient autoencoder structure. This approach not only minimizes the syntactic complexity by employing fewer neurons but also captures the semantic essence of the data. By learning the most influential neural structure with the fewest neurons, it can effectively model cardiovascular pressure-flow values. Furthermore, the incorporation of resistances and capacitances directly into the ''latent space'' enhances the accuracy and performance of the cardiovascular model. This streamlined representation of essential features yields a highly determinant model for the data. However, there are limitations, including reduced performance on learning data features due to the algorithm's dependence on the sequential order of time series data, which might not be optimal for comprehensive cardiovascular data. Future research will explore variational autoencoder structures and address challenges related to supervised learning for physiologically conscious neurons, aiming to improve the generation of physiological data within the proposed method.

Creating a controlled experimental environment with varying resistance and capacitance values to simulate clinical scenarios is challenging, as confirmed by previous research [36]. The presented method extensively examines aortic stenosis in four distinct phases, demonstrating the algorithm's capability to detect even subtle variations. While these conditions are manageable and reproducible in *in vitro* studies, identifying disease levels in experiments involving real tissues and human subjects remains notably complex [36]. This challenge extends to medical professionals, as clinical diagnosis of different disease levels is not straightforward [31]. Therefore, the direct evaluation of the presented algorithm's performance serves as a valuable contribution to the literature, offering a benchmark for future studies in this field.

Especially in the diagnosis of cardiovascular diseases, the advantages of the presented algorithm are considered significant. Aortic stenosis is a well-studied disease that has a significant impact on human life, and performing invasive tests for it is quite challenging. The presented hMCL and autoencoder algorithm aim to generate clinically accurate data for this disease, and the PCAE structure presented has been validated through in vitro studies. Mitral stenosis, on the other hand, is particularly difficult to study in the literature because simulating this disease is challenging both in living cells and in the laboratory environment. However, with PCAE, transient time responses and tests related to this disease can be conducted. The contractility, which is an indicator of heart stiffness, can be predicted with high precision using the presented PCAE structure, and new data can be simulated with high accuracy for other cardiovascular diseases.

The training model representation is very simple for which it may not handle complex non-linearity. It is observed that the 'attention-based autoencoder' structure is suitable for the intended tasks, especially for supervised learning [37]. However, making the necessary adjustments to modify the latent space with supervised learning would require defining a new cost function. Additionally, the proposed approach for closed-loop time response can effectively model physiological neurons in a simple and efficient manner.

On the other hand, the 'decision-tree' autoencoder structure is rule-based and can be effectively utilized in cardiovascular diagnostics [38]. Nevertheless, modifying the latent space and generating transient time states in the closed-loop response could be challenging. Therefore, using a variational autoencoder in future studies would be appropriate.

In order to improve the performance tests of the proposed method in clinical studies, it is necessary to conduct tests with non-invasively collected data, particularly testing Emax and ECG signals in the presented algorithm, and investigating its training performance. Furthermore, the presented algorithm is fed into the system with a delay to process time-series signals, which requires improvement in the algorithm depending on both the sampling frequency and the window interval. Additionally, while the performance of the presented framework has been validated through in vitro studies using data obtained from in silico simulations, it is essential to incorporate data from in vitro test results into the training process. However, this approach was avoided to demonstrate that the performance of the proposed method can be achieved not only in silico but also in untrained hMCL measurements.

V. CONCLUSION

In this study, a framework is propo8sed for estimating cardiovascular system (CVS) parameters based on principal variables derived from cardiovascular (CV) measurements. The framework utilizes both *in silico* (computer-simulated) and *in vitro* (laboratory) measurements and addresses various conditions such as aortic and mitral stenosis, left ventricle (LV) elastance deviation, and systemic resistance changes in four different severity levels.

At the core of the framework lies an autoencoder (AE) type of deep neural network. The AE is designed with a partially guided latent space, which is influenced by physiological parametric signals. The input to the AE consists of principal CV signals such as pressures and flow rates, while physiological consciousness is induced through critical CVS parameters that cannot be directly measured using non-invasive methods. These parameters include the aortic resistance, mitral resistance, systemic resistance, and left ventricle elastance.

The standard loss function of the AE is modified to enable specific neurons in the latent space to learn predefined CVS parameters. Training datasets are generated using *in silico* data obtained from a CVS model. To validate the proposed model, a hybrid mock loop device, constructed in-house, is used to collect corresponding CVS parameters and variables through *in vitro* tests.

The results of the *in vitro* tests demonstrate that the proposed deep neural network successfully predicts the principal CV variables and critical parameters with a mean error below 5.7% across a wide range of normal and abnormal conditions.

In addition to CVS parameter estimation, a diagnostics model is developed using only the latent space vector. This diagnostics model classifies CVS conditions into four severity levels. The overall F1 score, which measures the model's accuracy, for predicting all cardiovascular diseases (CVD) is reported as 98.55% for all cases studied.

The proposed framework proves to be effective in estimating CVS parameters and predicting CVS conditions in the four severity levels examined. The study suggests that the framework holds promise for extension to other cardiovascular conditions.

In future studies, performance tests of the proposed algorithm will be conducted by conditioning on the maximum elastance value of the left ventricle and the ECG signal which can noninvasively collected from the body. Particularly, the generation of time-series-based image content and the establishment of a variational autoencoder structure, along with the definition of a new cost function, aim to create a simulation framework using only ECG signals.

We will also add more CVD and expand the model to be a better assistant to cardiologists for their diagnostics and treatment strategies. Subsystems in the framework will also be implemented using transformers and CNNs. Clinical tests will be conducted to validate our findings.

REFERENCES

[1] World Health Organization. *Cardiovascular Diseases (CVDs)*. who.int. Accessed: Aug. 11, 2022. [Online]. Available: https://www.who.int/news-room/fact-sheets/detail/cardiovascular-diseases-(cvds)

[2] S. Romiti, M. Vinciguerra, W. Saade, I. A. Cortajarena, and E. Greco, "Artificial intelligence (AI) and cardiovascular diseases: An unexpected alliance," *Cardiol. Res. Pract.*, vol. 2020, pp. 1–8, Jun. 2020, doi: 10.1155/2020/4972346.

[3] J. Haas et al. *In Vivo Assay Guidelines (2012)*. Accessed: Aug. 15, 2022. http://www.ncbi.nlm.nih.gov/books/NBK92013/

[4] Y. Orime, S. Takatani, K. Tasai, Y. Ohara, K. Naito, K. Mizuguchi, K. Makinouchi, Y. Matsuda, T. Shimono, J. Glueck, G. P. Noon, and Y. Nosé, "In vitro and in vivo validation tests for total artificial heart," *Artif. Organs*, vol. 18, no. 1, pp. 54–72, Jan. 1994, doi: 10.1111/j.1525-1594.1994.tb03299.x.

[5] M. A. Simaan, A. Ferreira, S. Chen, J. F. Antaki, and D. G. Galati, "A dynamical state space representation and performance analysis of a feedback-controlled rotary left ventricular assist device," *IEEE Trans. Control Syst. Technol.*, vol. 17, no. 1, pp. 15–28, Jan. 2009, doi: 10.1109/TCST.2008.912123.

[6] S. Schampaert, K. A. M. A. Pennings, M. J. G. van de Molengraft, N. H. J. Pijls, F. N. van de Vosse, and M. C. M. Rutten, "A mock circulation model for cardiovascular device evaluation," *Physiolog. Meas.*, vol. 35, no. 4, pp. 687–702, Mar. 2014, doi: 10.1088/0967-3334/35/4/687.

[7] M. Abdi, A. Karimi, M. Navidbakhsh, G. P. Jahromi, and K. Hassani, "A lumped parameter mathematical model to analyze the effects of tachycardia and bradycardia on the cardiovascular system," *Int. J. Numer. Model., Electron. Netw., Devices Fields*, vol. 28, no. 3, pp. 346–357, Jul. 2014, doi: 10.1002/jnm.2010.

[8] M. Iscan and A. Yesildirek, "Novel aortic heart valve model parameterizing normal and pathological cases: Aortic stenosis and regurgitation," *Trans. Inst. Meas. Control*, 2023. [Online]. Available: https://journals.sagepub.com/doi/abs/10.1177/01423312231163363, doi: 10.1177/01423312231163363.

[9] K. R. Walley, "Left ventricular function: time-varying elastance and left ventricular aortic coupling," *Crit. Care*, vol. 20, no. 1, p. 270, Sep. 2016, doi: 10.1186/s13054-016-1439-6.

[10] M. Iscan and A. Yesildirek, "A new cardiovascular mock loop driven by novel active capacitance in normal and abnormal conditions," *Appl. Bionics Biomechanics*, Oct. 2023, doi: 10.1155/1970/2866637.

[11] J. N. Warnock, S. Konduri, Z. He, and A. P. Yoganathan, "Design of a sterile organ culture system for the ex vivo study of aortic heart valves," *J. Biomech. Eng.*, vol. 127, no. 5, pp. 857–861, Oct. 2005, doi: 10.1115/1.1992535.

[12] E. S. Rapp, S. R. Pawar, and R. G. Longoria, "Hybrid mock circulatory loop simulation of extreme cardiac events," *IEEE Trans. Biomed. Eng.*, vol. 69, no. 9, pp. 2883–2892, Sep. 2022, doi: 10.1109/TBME.2022.3156963.

[13] E. Vignali, E. Gasparotti, A. Mariotti, D. Haxhiademi, L. Ait-Ali, and S. Celi, "High-versatility left ventricle pump and aortic mock circulatory loop development for patient-specific hemodynamic in vitro analysis," *ASAIO J.*, vol. 68, no. 10, pp. 1272–1281, Oct. 2022, doi: 10.1097/MAT.0000000000001651.

[14] M. Swathy and K. Saruladha, "A comparative study of classification and prediction of cardio-vascular diseases (CVD) using machine learning and deep learning techniques," *ICT Exp.*, vol. 8, no. 1, pp. 109–116, Mar. 2022, doi: 10.1016/j.icte.2021.08.021.

[15] R. G. Nadakinamani, A. Reyana, S. Kautish, A. S. Vibith, Y. Gupta, S. F. Abdelwahab, and A. W. Mohamed, "Clinical data analysis for prediction of cardiovascular disease using machine learning techniques," *Comput. Intell. Neurosci.*, vol. 2022, pp. 1–13, Jan. 2022, doi: 10.1155/2022/2973324.

[16] A. Shimazaki, D. Ueda, A. Choppin, A. Yamamoto, T. Honjo, Y. Shimahara, and Y. Miki, "Deep learning-based algorithm for lung cancer detection on chest radiographs using the segmentation method," *Sci. Rep.*, vol. 12, no. 1, p. 727, Jan. 2022, doi: 10.1038/s41598-021-04667-w.

[17] S. Sanchez-Martinez, O. Camara, G. Piella, M. Cikes, M. Á. González-Ballester, M. Miron, A. Vellido, E. Gómez, A. G. Fraser, and B. Bijnens, "Machine learning for clinical decision-making: Challenges and opportunities in cardiovascular imaging," *Frontiers Cardiovascular Med.*, vol. 8, Jan. 2022, Art. no. 765693, doi: 10.3389/fcvm.2021.765693.

[18] Y. Zhou, Y. He, J. Wu, C. Cui, M. Chen, and B. Sun, "A method of parameter estimation for cardiovascular hemodynamics based on deep learning and its application to personalize a reduced-order model," *Int. J. Numer. Methods Biomed. Eng.*, vol. 38, no. 1, Jan. 2022, Art. no. e3533, doi: 10.1002/cnm.3533.

[19] V. Bikia, S. Pagoulatou, B. Trachet, D. Soulis, A. D. Protogerou, T. G. Papaioannou, and N. Stergiopulos, "Noninvasive cardiac output and central systolic pressure from cuff-pressure and pulse wave velocity," *IEEE J. Biomed. Health Informat.*, vol. 24, no. 7, pp. 1968–1981, Jul. 2020, doi: 10.1109/JBHI.2019.2956604.

[20] J. Bonnemain, M. Zeller, L. Pegolotti, S. Deparis, and L. Liaudet, "Deep neural network to accurately predict left ventricular systolic function under mechanical assistance," *Frontiers Cardiovascular Med.*, vol. 8, Oct. 2021, Art. no. 752088, doi: 10.3389/fcvm.2021.752088.

[21] R. Laubscher, J. Van Der Merwe, P. Herbst, and J. Liebenberg, "Estimation of simulated left ventricle elastance using lumped parameter modelling and gradient-based optimization with forward-mode automatic differentiation based on synthetically generated noninvasive data," *J. Biomech. Eng.*, vol. 145, no. 2, Feb. 2023, Art. no. 021008, doi: 10.1115/1.4055565.

[22] S. R. Pawar, E. S. Rapp, J. R. Gohean, and R. G. Longoria, "Parameter identification of cardiovascular system model used for left ventricular assist device algorithms," *J. Eng. Sci. Med. Diag. Therapy*, vol. 5, no. 1, Feb. 2022, Art. no. 011006, doi: 10.1115/1.4053065.

[23] Y. Dabiri, A. Van Der Velden, K. L. Sack, J. S. Choy, G. S. Kassab, and J. M. Guccione, "Prediction of left ventricular mechanics using machine learning," *Frontiers Phys.*, vol. 7, p. 117, Sep. 2019, doi: 10.3389/fphy.2019.00117.

[24] X. Yang, J. S. Leandro, T. D. Cordeiro, and A. M. N. Lima, "An inverse problem approach for parameter estimation of cardiovascular system models," in *Proc. 43rd Annu. Int. Conf. IEEE Eng. Med. Biol. Soc. (EMBC)*, Nov. 2021, pp. 5642–5645, doi: 10.1109/EMBC46164.2021.9629603.

[25] E. S. Rapp, S. R. Pawar, J. R. Gohean, E. R. Larson, R. W. Smalling, and R. G. Longoria, "Estimation of systemic vascular resistance using built-in sensing from an implanted left ventricular assist device," *J. Eng. Sci. Med. Diag. Therapy*, vol. 2, no. 4, Nov. 2019, Art. no. 041008, doi: 10.1115/1.4045204.

[26] V. Bikia, M. Lazaroska, D. Scherrer Ma, M. Zhao, G. Rovas, S. Pagoulatou, and N. Stergiopulos, "Estimation of left ventricular end-systolic elastance from brachial pressure waveform via deep learning," *Frontiers Bioeng. Biotechnol.*, vol. 9, Oct. 2021, Art. no. 754003, doi: 10.3389/fbioe.2021.754003.

[27] D. P. Stonko, J. Edwards, H. Abdou, N. N. Elansary, E. Lang, S. G. Savidge, and J. J. Morrison, "A technical and data analytic approach to pressure-volume loops over numerous cardiac cycles," *JVS-Vascular Sci.*, vol. 3, pp. 73–84, Jan. 2022, doi: 10.1016/j.jvssci.2021.12.003.

[28] B. A. Olshausen and D. J. Field, "Sparse coding with an overcomplete basis set: A strategy employed by V1?" *Vis. Res.*, vol. 37, no. 23, pp. 3311–3325, Dec. 1997, doi: 10.1016/S0042-6989(97)00169-7.

[29] X. Li, L. Yu, D. Chang, Z. Ma, and J. Cao, "Dual cross-entropy loss for small-sample fine-grained vehicle classification," *IEEE Trans. Veh. Technol.*, vol. 68, no. 5, pp. 4204–4212, May 2019, doi: 10.1109/TVT.2019.2895651.

[30] Y. N. V. Reddy, J. P. Murgo, and R. A. Nishimura, "Complexity of defining severe 'stenosis' from mitral annular calcification," *Circulation*, vol. 140, no. 7, pp. 523–525, Aug. 2019, doi: 10.1161/CIRCULATIONAHA.119.040095.

[31] F. M. Colacino, F. Moscato, F. Piedimonte, G. Danieli, S. Nicosia, and M. Arabia, "A modified elastance model to control mock ventricles in real-time: Numerical and experimental validation," *ASAIO J.*, vol. 54, no. 6, pp. 563–573, Nov. 2008, doi: 10.1097/MAT.0b013e31818a5c93.

[32] S. D. Gregory, M. Stevens, D. Timms, and M. Pearcy, "Replication of the frank-starling response in a mock circulation loop," in *Proc. Annu. Int. Conf. IEEE Eng. Med. Biol. Soc.*, Aug. 2011, pp. 6825–6828, doi: 10.1109/IEMBS.2011.6091683.

[33] B. W. Matthews, "Comparison of the predicted and observed secondary structure of T4 phage lysozyme," *Biochim. Biophys. Acta-Protein Struct.*, vol. 405, no. 2, pp. 442–451, Oct. 1975, doi: 10.1016/0005-2795(75)90109-9.

[34] M. L. McHugh, "Interrater reliability: The Kappa statistic," *Biochemia Medica*, vol. 22, pp. 276–282, Oct. 2012, doi: 10.11613/BM.2012.031.

[35] F. Regazzoni, M. Salvador, L. Dede', and A. Quarteroni, "A machine learning method for real-time numerical simulations of cardiac electromechanics," *Comput. Methods Appl. Mech. Eng.*, vol. 393, Apr. 2022, Art. no. 114825, doi: 10.1016/j.cma.2022.114825.

[36] M. Rocchi, M. Ingram, P. Claus, J. D'hooge, B. Meyns, and L. Fresiello, "Use of 3D anatomical models in mock circulatory loops for cardiac medical device testing," *Artif. Organs*, vol. 47, no. 2, pp. 260–272, Feb. 2023, doi: 10.1111/aor.14433.

[37] N. Aslam, P. K. Rai, and M. H. Kolekar, "A3N: Attention-based adversarial autoencoder network for detecting anomalies in video sequence," *J. Vis. Commun. Image Represent.*, vol. 87, Aug. 2022, Art. no. 103598, doi: 10.1016/j.jvcir.2022.103598.

[38] D. L. Aguilar, M. A. Medina-Pérez, O. Loyola-González, K.-K.-R. Choo, and E. Bucheli-Susarrey, "Towards an interpretable autoencoder: A decision-tree-based autoencoder and its application in anomaly detection," *IEEE Trans. Depend. Secure Comput.*, vol. 20, no. 2, pp. 1048–1059, Mar. 2023, doi: 10.1109/TDSC.2022.3148331.

MEHMET ISCAN received the B.S. and M.S. degrees in mechatronic engineering from Yıldız Technical University, Turkey, in 2013 and 2016, respectively, where he is currently pursuing the Ph.D. degree. He is a Research Assistant with Yıldız Technical University. He is also the Co-Founder of Phinite Technology Corporation, a biomedical company developing cardiac testing devices and Holter. His research interests include mechatronic design, neural networks, and the detection of cardiac abnormalities.

AYDIN YESILDIREK (Member, IEEE) received the B.S. degree in electronics engineering from the Technical University of Istanbul, in 1986, the M.S. degree in electrical engineering and applied science from Case Western Reserve University, Cleveland, OH, USA, in 1992, and the Ph.D. degree in electrical engineering from The University of Texas at Arlington, Arlington, TX, USA, in 1994. In 1995, he joined Idaho State University, Pocatello, ID, USA, as a Postdoctoral Fellow. From 1996 to 1999, he was the Manager of the Research and Development Department, VGT, Panama City, Panama. In 1999, he joined the Department of Electrical and Computer Engineering, Gannon University, Erie, PA, USA, as an Assistant Professor, till 2007. From 2007 to 2014, he was an Associate Professor with the Department of Electrical Engineering, American University of Sharjah, United Arab Emirates. Since 2014, he has been with the Department of Mechatronics Engineering, Yıldız Technical University, Istanbul, Turkey. His research interests include autonomous robotics, intelligent control, modeling and analysis of biomedical systems using artificial intelligence, and deep learning framework.

• • •